Biosensors and Bioelectronics 98 (2017) 330–337

Contents lists available at ScienceDirect

Biosensors and Bioelectronics

journal homepage: www.elsevier.com/locate/bios

Electrochemical peptide sensor for diagnosing adenoma-carcinoma transition in colon cancer

Jong Min Lim[a,1], Myung Yi Ryu[a,1], Jong Won Yun[b], Tae Jung Park[c], Jong Pil Park[a,*]

[a] Department of Pharmaceutical Engineering, Daegu Haany University, Gyeongsan 38610, Republic of Korea
[b] Department of Biotechnology, Daegu University, Gyeongsan 38453, Republic of Korea
[c] Department of Chemistry, Institute of Interdisciplinary Convergence Research, Research Institute of Halal Industrialization Technology, Chung-Ang University, 84 Heukseok-ro, Dongjak-gu, Seoul 06974, Republic of Korea

ARTICLE INFO

Keywords:
Colon cancer
LRG1
Affinity peptide
Sensitivity
Electrochemical sensor

ABSTRACT

Colorectal cancer (CRC) is one of the leading causes of cancer-related deaths. Therefore, more sensitive and early diagnostic methods for CRC are urgently needed. In this study, an efficient electrochemical biosensor for early diagnosis of adenoma-to-carcinoma progression that employs a series of chemically modified affinity peptides was developed. A series of amino acid-substituted and cysteine-incorporated synthetic peptides with flexible linkers was chemically synthesized and immobilized to a gold sensor layer; performance of the sensor was monitored using cyclic voltammetry (CV) and electrochemical impedance spectroscopy (EIS). Potential affinity peptides (LRG1 BP1–BP4) specific for the LRG1 biomarker as a target protein were chosen according to a quantitative current decrease and dynamic impedance increase by CV and EIS, respectively. Using EIS, the K_d value of the LRG1 BP3 peptide was found to be 8.3 ± 2.7 nM. The applicability of the sensor to detect LRG1 proteins was confirmed in human plasma from colorectal adenomas and carcinomas (n = 20 in each group). The detection of LRG1 in accordance with the ΔR_{ct} value (electron-transfer resistance at the electrode surface) of the sensor layer incorporating LRG1 BP3 peptides showed a statistically significant difference ($p < 0.001$) between adenomas and carcinomas, indicating that the potential use of this biosensing platform for detecting the CRC biomarker, as well as for monitoring the colorectal adenoma-to-carcinoma transition in an electrochemically miniaturized biosensor (*e*-chem biosensor) in point-of-care testing, is possible.

1. Introduction

Colon cancer, a malignant cancer arising in the large intestine, is one of the most common cancers and is the third leading cause of death worldwide (Choi et al., 2013; Galamb et al., 2009; Sole et al., 2014; Zhang et al., 2007). Several clinical diagnostic methods are commonly used for the early detection of colorectal cancer (CRC), including sigmoidoscopy or virtual colonoscopy with biopsy confirmation of cancer tissue and blood (Choi et al., 2013; Galamb et al., 2009; Wu and Qu, 2015). Although miniaturized colonomicroscopy is the most powerful method for early diagnosis of CRC in hospitals, it requires multi-step processing with unfavorable conditions for the patients, requiring lengthy clinical processes. This technique also involves relatively high medical cost and invasive methods, and presents a small risk of perforation in the wall of the colon, though this statistical possibility is quite rare (Galamb et al., 2009; Kumar et al., 2011). Thus, there has been an increasing demand for the development of new diagnostic techniques that are capable of rapid and precise detection of cancer targets. Toward this goal, non-invasive and multi-functional diagnostic methods for the efficient prediction of early-stage CRC or pre-malignant lesions are being developed (Abdolahad et al., 2014; Albrethsen et al., 2005; Choi et al., 2013; Galamb et al., 2009; Kolitz-Domb et al., 2014; Schoen, 2002; Yi et al., 2012; Zhang et al., 2007). For example, a PCR-based assay (Clark-Langone et al., 2007; Galamb et al., 2009), a gene mutation assay (Yi et al., 2012), an antibody-based assay (Tao et al., 2012), and a biomarker-based method (Li et al., 2013) have been developed. However, these methods still possess some challenges for becoming ready-to-use in the early diagnosis of CRC. Recently, promising biomarkers from human plasma or blood suitable for diagnosing CRC have been proposed and well-characterized (Choi et al., 2013; Giusti et al., 2012; Ihi et al., 1997; Rangiah et al., 2009; Sole et al., 2014; Wu and Qu, 2015; Yi et al., 2012). Choi et al. (2013) reported that leucine-rich α-2-glycoprotein 1 (LRG1) was highly over-expressed up to a 2-fold increase in CRC patients. According to their

* Corresponding author.
E-mail address: jppark@dhu.ac.kr (J.P. Park).
[1] These authors contributed equally to this study.

http://dx.doi.org/10.1016/j.bios.2017.07.013
Received 26 March 2017; Received in revised form 1 July 2017; Accepted 5 July 2017
Available online 06 July 2017
0956-5663/ © 2017 Elsevier B.V. All rights reserved.

studies, LRG1 may play an important role in apoptosis and cell survival. Additionally, the level of LRG1 in plasma from CRC patients was well-correlated with the progression of CRC from the adenoma to carcinoma stage. Furthering these findings, we have recently reported that unique and short linear affinity peptides specific for the target protein LRG1 were identified by an M13 phage display technique; their relative binding affinities were characterized by an enzyme-linked immunosorbent assay (ELISA) (Hwang et al., 2016). From these results, we observed that the phage-displayed peptides displayed sub-picomolar binding affinities for LRG1 proteins.

Affinity reagents that specifically bind to antigens are very important molecules in clinical and diagnostic applications. In particular, antibodies are the key reagents in many important fields, such as diagnosis of various diseases, therapeutics, and clinical or pharmaceutical analysis. Polyclonal antibodies are relatively cost-effective but possess heterogeneous binding properties, while monoclonal antibodies are expensive to produce from animal cells, but are homogeneous with high specificity (Hwang et al., 2015; Park et al., 2010, 2015; Wu et al., 2011). Antibody-like molecules such as single-chain fragment variables (scF_v) and fragment antigen binding (F_{ab}) are also promising alternatives monoclonal antibodies (Crivianu-Gaita and Thompson, 2016). Comparatively, aptamers have also been studied in biosensor development. Most aptamers are single-stranded nucleic acids that are identified using combinatorial techniques (e.g. SELEX) and selectively bind to various target molecules (Crivianu-Gaita and Thompson, 2016; Hu et al., 2014).

Current immunoassays rely mainly on antibodies as affinity reagents, are relatively expensive, require multiple sample preparations (Hwang et al., 2015; Park et al., 2010, 2015), and sometimes lead to false-positive results. Compared to the use of antibodies, linear and unique short peptides have attracted attention as effective affinity reagents in the development of new biosensors (Wu et al., 2011). One of the most exciting properties of the peptides is their small size and cost efficiency in the creation of a new biosensing platform (Hwang et al., 2016; Park et al., 2015). Generally, peptides are either linear or in a cyclic form, indicating that peptides are more amenable than antibodies to engineering at the molecular level. In addition, targeting peptides can be attached easily to the surfaces of materials such as nanoparticles or liposomes for bio-imaging and new bioassay systems (Wu et al., 2010, 2011).

The evolutionary M13 phage display technique is widely utilized for identifying unique affinity peptides that selectively bind to nearly limitless targets (Kehoe and Kay, 2005). This procedure includes the following steps: i) the phage displaying peptide interacts with the chosen targets, and unbound phages are washed away; ii) bound phages are eluted at low pH (pH 2.2), neutralized, and then amplified in *E. coli*; iii) the individual phage clones are sequenced, and a phage ELISA is performed. There have been some reports in which the entire phage clones, or the free peptides identified from these selections, were used as recognition elements on various types of biosensors (Hwang et al., 2017, 2015; Sidhu, 2001). Using this strategy, our group has recently reported a new biosensor for detecting troponin I (a cardiac biomarker) (Park et al., 2010), norovirus (foodborne pathogen) (Hwang et al., 2017), procalcitonin (a kidney biomarker) (Park et al., 2015), alanine aminotransferase (a liver function biomarker) (Wu et al., 2011), and a CRC biomarker (Hwang et al., 2016).

Meanwhile, a number of remarkable electrochemical detection platforms have been developed for clinical and bioanalytical applications (Abdolahad et al., 2014; Hwang et al., 2017; Wu et al., 2010). Among electrochemical sensing methods, cyclic voltammetry (CV) and electrochemical impedance spectroscopy (EIS)-based detections have been widely used because they have the potential for rapid response, label-free detection, and robust reliability (Hwang et al., 2017; Wu et al., 2011). Both methods can measure either the change of current or the impedance by applying voltage. When applied on an electrode, the method measures binding of molecules on the electrode layer by mass adsorption which obstruct the access of an electroactive redox probe to the electrode, therefore decreasing the redox current in CV or increase impedance in EIS. Additionally, one of the exciting benefits of these approaches is that they do not require labeling for detection. However, there are some considerations for aspects further refinements (Daniels and Pourmand, 2007). For example, the size of the electrode can affect the actual impedance and can be chosen with respect to instrument's frequency range. Increasing frequency will be less affected by drift and noise in the measurement. In addition, reduction of the electrode area or thickness may also affect impedance change upon target binding. In this study, we demonstrate the first use of synthetic affinity peptides identified through phage display for the development of an electrochemical biosensor toward the early diagnosis of CRC from plasma in patients with both adenoma and carcinoma. The basic principle of our study is as follows; once the most promising affinity peptide for target was selected, a cysteine-incorporated peptide was chemically synthesized and transferred to the gold electrode. Thereafter, the peptide-modified gold electrode was used to detect LRG1 and evaluated the performance of the sensor using CV and EIS.

2. Materials and methods

2.1. Chemicals

Bovine serum albumin (BSA) was purchased from Sigma-Aldrich (St. Louis, MO, USA). Human recombinant LRG1 proteins were purchased from Randox Life Science (Crumlin, UK). A series of synthetic peptides modified with a C-terminal cysteine and a flexible linker (-GGGGS-) were chemically synthesized (> 95% purity) by Peptron (Daejeon, Korea), as shown in Table S1. The quartz crystals deposited with gold were obtained from Biolin Scientific (Stockholm, Sweden). Phosphate-buffered saline (PBS, pH 7.4) and Tris-HCl buffer solutions were used to make all proteins, human plasma samples, and synthetic peptide solutions for CV and EIS measurements. Unless otherwise stated, all reagents were analytical grade.

2.2. Preparation of human patient plasma samples

A total of 40 patients with adenomas (n = 20) and carcinomas (n = 20) were used (Table S2). The study protocol was reviewed and approved by the College of Medicine, Keimyung University. In detail, blood samples from the two groups were collected, and then the crude blood plasma was separated by centrifugation (3,000×g, 10 min), as demonstrated previously (Choi et al., 2013). Finally, the fractionated plasma was directly used for electrochemical analysis without any purification.

2.3. Circular dichroism (CD) spectroscopy

Circular dichroism (CD) spectra of all synthetic peptides at a concentration of 50 μM were recorded on a CD spectrometer (J-715, JASCO, Tokyo, Japan) using a UV cell with 0.1 cm optical path length at 25 °C. For the CD analysis, PBS solution (pH 7.4) was used, and CD spectra were scanned 4 times for every sample, as previously reported (Hwang et al., 2017).

2.4. Preparation of the affinity peptide-modified electrode

The peptide-functionalized gold electrode (14 × 20 mm in size) was prepared by the following steps. First, the gold electrode was immersed into piranha solution (H_2SO_4:H_2O_2 = 4:1, v/v) for 10 min to remove residual dust and impurities on the surface layer of the gold electrode. The electrode was then rinsed with deionized (DI) water several times. This pre-functionalized electrode was dried by blowing with N_2 gas for several seconds. After these polishing steps, the electrode and voltammetric cell were assembled, and 100 μL of thiol-modified synthetic

peptides (50 μg/mL) were dropped onto the gold electrode and incubated at room temperature for 1 h. To remove unbound synthetic peptides, the cell was washed with 1X PBS (pH 7.4) and then again with DI water. Next, 2 μL of pure LRG1 proteins or human plasma samples was loaded onto each assembled cell and then incubated at room temperature for 1 h. The cells were again sequentially washed with 1X PBS and DI water to remove the unbound proteins.

2.5. CV and EIS measurements

A conventional three-electrode system, including a working electrode, platinum counter electrode, and Ag/AgCl reference electrode, was used for the electrochemical measurements. CV and EIS were performed using an electrochemical analyzer (CHI 750E, CH Instruments, Austin, TX) connected to a computer data analysis system. These analyses were conducted in a PBS solution with 4 mM ferro/ferricyanide, as described in our previous study (Hwang et al., 2017). The CV was recorded from 0.0 V to +0.4 V vs. an Ag/AgCl electrode at a sweep rate of 20 mV/s. EIS was carried out at a formal DC potential of 0.2 V using an alternating voltage of 10 mV in the frequency range from 10 Hz to 10 kHz.

2.6. Statistical analysis

A two-way analysis of variance (ANOVA) was used to determine the significance of the cross-reactivity of the binding peptides, as well as the effects of the crude human plasma (GraphPad Software Inc., La Jolla, CA, USA). A Student's *t*-test was used to compare the electron-transfer resistance at the electrode surface, ΔR_{ct}. In all cases, a value of $p < 0.001$ was considered significant.

3. Results and discussion

3.1. Rational design and synthesis of affinity peptides

As mentioned above, we have reported the first study that identifies and characterizes unique affinity peptides that selectively bind to the CRC biomarker LRG1 protein (Hwang et al., 2016). We learned from this study that the phage-displayed peptides had nanomolar affinity for LRG1 protein. Thus, the free peptides separated from the phage particles may provide new opportunities for the creation of an electrochemical sensor toward the early diagnosis of CRC. To evaluate our hypothesis, a series of synthetic peptides specific for LRG1 proteins identified from the M13 phage display technique was chemically synthesized with a cysteine residue (Cys) at the C-terminus to form a thiol self-assembled monolayer on a gold surface layer and a flexible linker (-GGGGS-) for molecular flexibility. The binding events were subsequently monitored in situ by CV and EIS. The sequences of synthetic peptides used in this study, and their characteristics are shown in Table S1. First, LRG1 BP1, which was identified from phage particles, was used as a scaffold to progressively create analogs of other peptides and had an amino acid sequence of QHIMHLPHINTLGGGGSC. Second, LRG1 BP2 peptide, which was made by substituting Ser for Ile at positions 3 and 9, Gln for Met at position 4, and Thr for Leu at position 6 in LRG1 BP1, was created to evaluate the effects of neutral amino acid residues on binding interactions. It had an amino acid sequence of QHSQHTPHSNTTGGGGSC. Third, LRG1 BP3 was made by substituting Asp for His at positions 2, 5, and 8 in LRG1 BP1 to investigate the effects of negatively charged amino acid residues on binding interactions. It had an amino acid sequence of QDIMDLPDINTLGGGGSC. Finally, the importance of the proline hinges was also investigated using LRG1 BP4, in which Phe was replaced with Pro at position 7 in LRG1 BP1. It had an amino acid sequence of QHIMHLFHINTLGGGGSC.

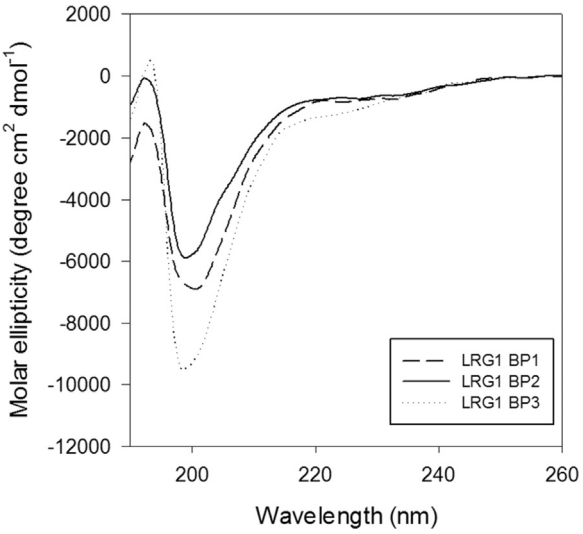

Fig. 1. Structural analysis of synthetic affinity peptides. Scans were carried out on 50 μM of each peptide described in the Section 2.

3.2. Analysis of the secondary structure of affinity peptides

To analyze the secondary structure of synthetic peptides and its structural insights on binding interactions, four analogs of LRG1 BP1 were analyzed by CD spectroscopy. In a sequence analysis, LRG1 BP1 was used as a peptide scaffold for the rational design of affinity peptides for the creation of an electrochemical biosensor. Sequence analysis revealed that it was rich in basic and hydrophobic uncharged residues (3 basic His residues, and uncharged hydrophobic residues including Ile, Met, Leu, and Pro). The pI value (isoelectric point) of LRG1 BP1 was predicted to be about 7.61. In the case of LRG1 BP2, which contains mostly neutral amino acid residues, the empirical pI value was 7.62. The pI value of the negatively charged LRG1 BP3 was 3.34, and that of LRG1 BP4 – the proline-containing analog – was 7.62.

The molar ellipticity values of LRG1 BP1–BP3 peptides indicated similar random coil structures, although not identical (Fig. 1). The secondary structural analysis of LRG1 BP1 revealed α-helix (4.6%), β-sheet (37.7%), and β-turn (14%), while analysis of LRG1 BP2 indicated α-helix (4.1%), β-sheet (38.7%), and β-turn (13.9%). In the case of LRG1 BP3, 5% of α-helix, 36.1% of β-sheet, and 14% of β-turn were observed. Unfortunately, no reliable CD spectrum of LRG1 BP4 could be obtained, possibly due to the limited presence of salts or Cl^- ions in the peptide sample.

3.3. Screening of synthetic peptides specific for detection of LRG1 proteins

To determine the best synthetic peptides specific to LRG1 proteins, the relative binding affinities of four peptide analogs (LRG1 BP1–BP4) were compared by CV (Fig. 2) and EIS measurements (Fig. 3). The binding affinities of the series of synthetic peptides were determined by comparing the interactions of LRG1 proteins with the peptides on a pre-immobilized gold surface layer and were observed as a change in current and impedance using CV and EIS, respectively. Among the peptides, LRG1 BP3 resulted in both the greatest decrease in current and increase in impedance. The presence of LRG1 proteins at varying concentrations appears to further the quantitative decrease of the CV signal and increase of impedance in EIS due to mass loading and specific recognition of other proteins. In the CV measurements, when we monitored the change of current and impedance before and after protein binding, a linear correlation was observed between the decreases in CV and the increases in EIS in the presence of proteins. In fact, the relative binding affinity of the peptides followed the trend

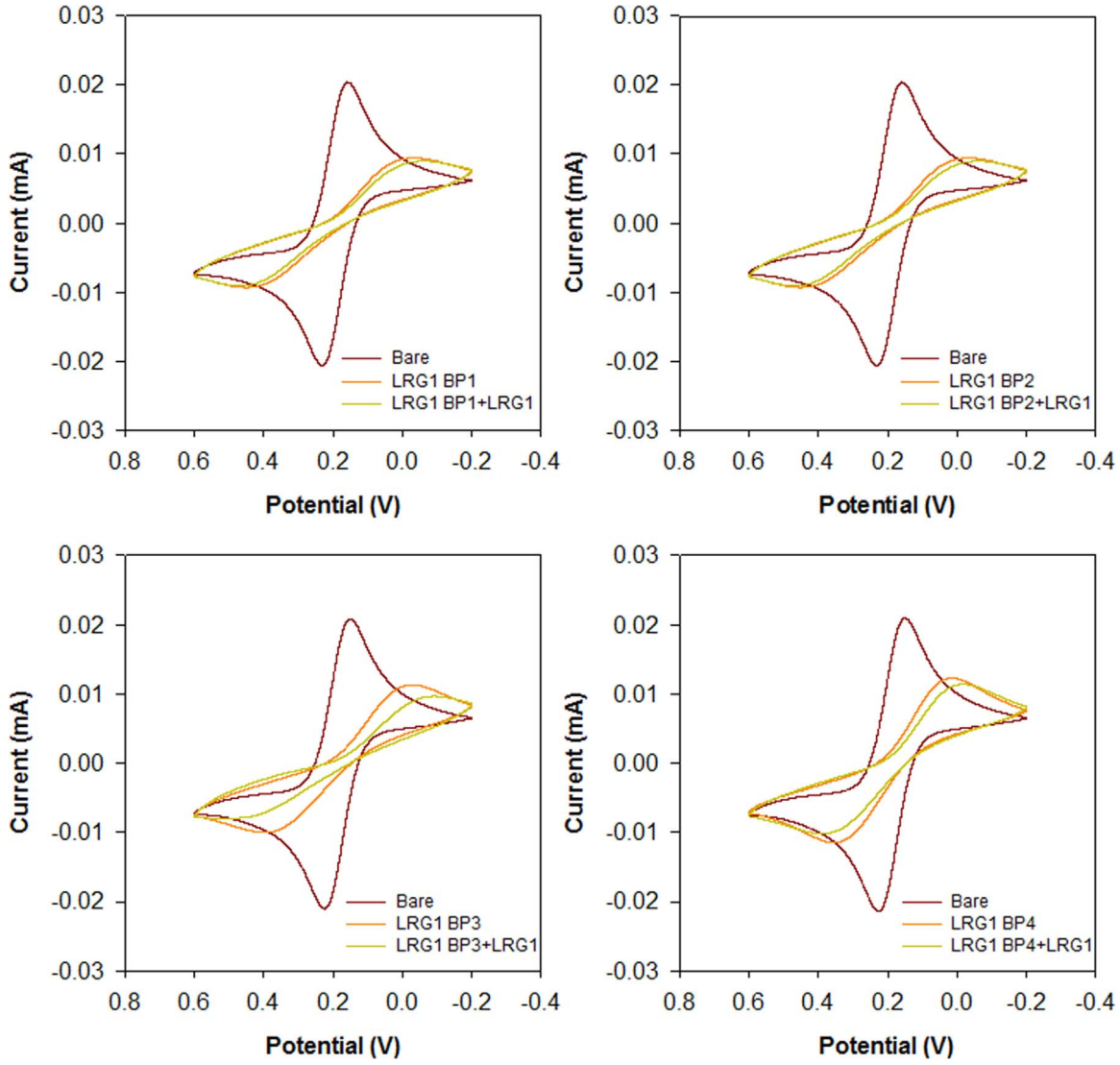

Fig. 2. Relative binding affinities of four synthetic peptides (LRG1 BP1–BP4) by CV for LRG1 proteins.

LRG1 BP3 > LRG1 BP1 > LRG1 BP4 > LRG1 BP2. These results indicated successful immobilization of the peptides and binding of proteins on the sensor layer, providing sensitive affinity for LRG1 proteins. From these observations, we chose LRG1 BP3 as a potential affinity peptide for the detection of target proteins. It is noteworthy that LRG1 BP3 peptide is able to form a random coil structure and has both negatively charged and neutral amino acid residues, such as Gln at position 1 and Asp at positions 2, 5, and 8. It also has one Pro residue at position 7, indicating that a structural and/or flexible link may be required for efficient binding of targets. These features suggested that a net negative charge with low pI and neutral amino acid residues may be dominant factors for binding of LRG1 proteins.

3.4. Optimization of LRG1 BP3 peptide concentrations on binding interactions using EIS

After selecting the best peptide, we investigated the effects of synthetic peptide concentrations on binding events toward the detection of LRG1 proteins on our sensor system. A dynamic response using LRG1 BP3 affinity peptides on a gold electrode layer was measured before and after incubation with LRG1 proteins (10 μg/mL). The R_{ct} (electron-transfer resistance) signal increased with increasing amounts of target proteins and reached saturation at 50 μg/mL, the concentration at which the signal leveled off. Therefore, a concentration of 50 μg/mL of LRG1 BP3 peptide was selected for further experiments (Fig. 4a). This phenomenon is not surprising, and is actually consistent with our previous study (Wu et al., 2011). In general, an EIS spectrum is commonly represented as a Nyquist plot with Z' versus Z'', where Z' and Z'' are the real and imaginary parts, respectively. It is known that a Randles circuit is the simplest model that defines the R_{ct} value, which is approximately equal to the diameter of the plotted semi-circle. In general, the Warburg impedance (W) results from the diffusion of ions, and it can reflect the property of the bulk solution. However, double layer capacitance (C_{dl}) is formed as ions from the solution absorbed onto the electrode surface because the electrode is polarized relative to the solution, it attracts ions of opposite charge (Daniels and Pourmand, 2007). In our system, Warburg impedance and ionic double layer capacitance can affect the performance of the sensor system; however, it may play a minor role in the overall measured impedance. When the analyte is bound on a functionalized electrode surface layer, hindrance of the redox probe will cause a bigger Nyquist semi-circle. Therefore, a larger semi-circle indicates a larger R_{ct} value. The change in the relative R_{ct} signal corresponding to the binding of LRG1 proteins to synthetic peptides was calculated by the following equation (Grewal et al., 2014):

$$\Delta R_{ct} = (R_{ct,\ protein} - R_{ct,\ peptide})/R_{ct,\ peptide} \times 100$$

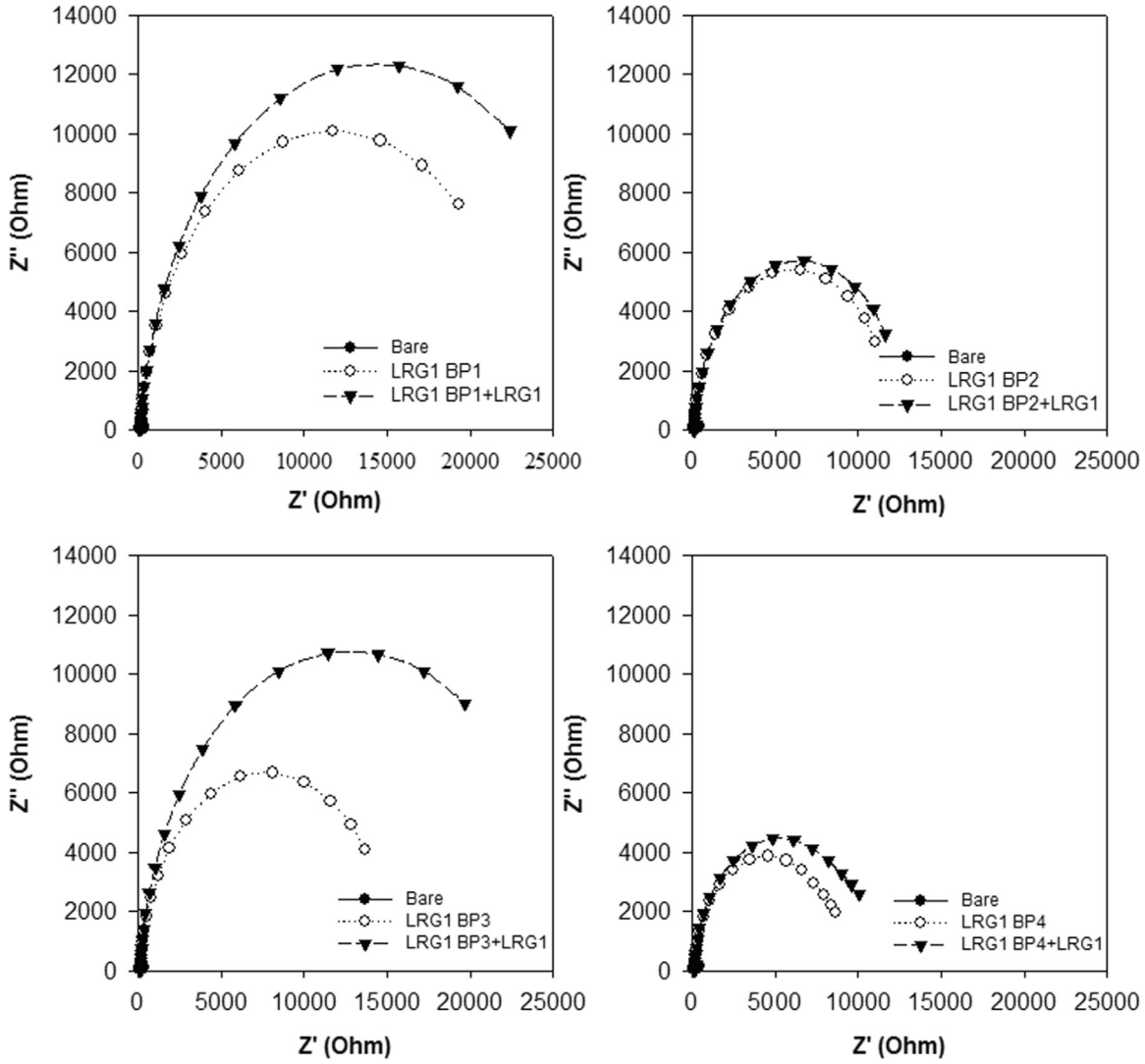

Fig. 3. Relative binding affinities of four synthetic peptides (LRG1 BP1–BP4) by EIS for LRG1 proteins. The value of R_{ct} of bare electrode in each measurement with BP1-BP4 is 80 Ω, 115 Ω, 90 Ω and 95 Ω, respectively.

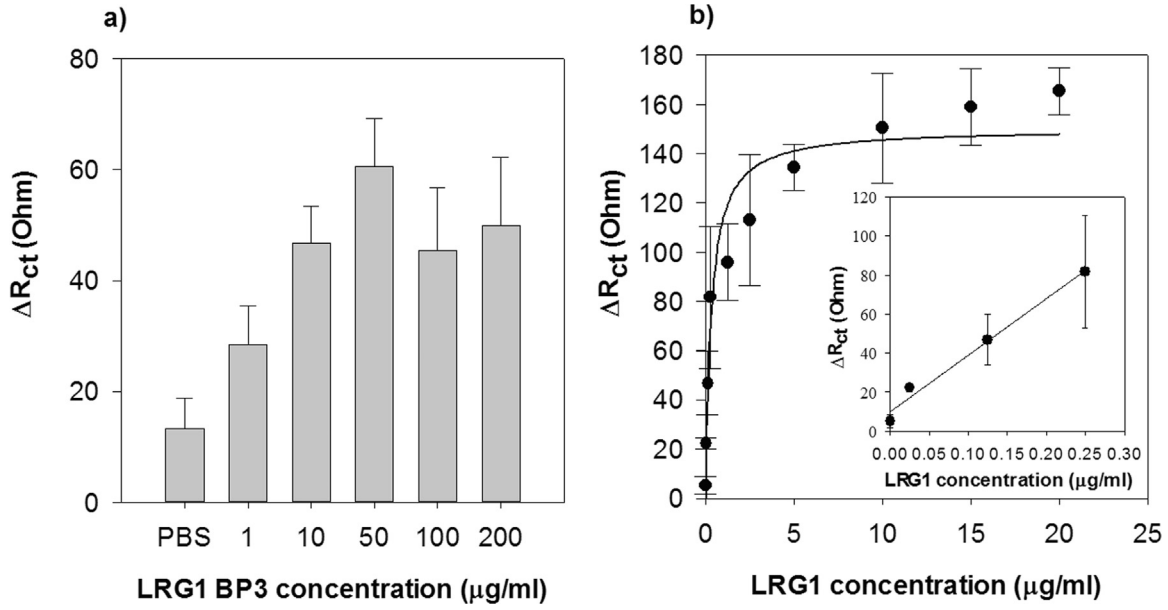

Fig. 4. Optimization of LRG1 BP3 peptide concentration on binding interactions (a) and dynamic response curve of LRG1 protein binding on gold-immobilized peptides (b). (inset, plot for lower (0–0.25 μg/mL) concentration. All measurements were done in triplicate, and error bars represent standard deviations.

where, $R_{ct,\ peptide}$ was the mean value of R_{ct} after immobilizing peptides only (no addition of target protein), and $R_{ct,\ protein}$ was the mean value of R_{ct} after addition of the target proteins. No dynamic response for PBS buffer as a control was observed.

3.5. Optimization of LRG1 protein concentrations on binding interactions using CV and EIS

To further optimize the LRG1 protein concentration with respect to binding interactions, 50 μg/mL of LRG1 BP3 with LRG1 protein concentrations ranging from 0.0025 μg/mL to 20 μg/mL was incubated on the gold surface layer; the current and impedance changes were then monitored by CV and EIS, respectively. The immobilization of LRG1 BP3 peptides resulted in an impedance increase by EIS due to surface blocking. The mean value of R_{ct} determined by EIS increased in a concentration-dependent manner and reached saturation at 10 μg/mL.

From the competition curve data (Fig. 4b), the dissociation binding constants (K_d) of the LRG1 BP peptides was were analyzed by non-linear regression. The K_d value was found to be 0.32 μg/mL (8.3 ± 2.7 nM) for LRG1 proteins and statistically significantly different using a Student's *t*-test ($p < 0.001$). It is noteworthy that the newly identified LRG1 BP3 peptides had an limit of detection (LOD) of 0.025 μg/mL, which is near the normal level of LRG1 in adenoma and carcinoma plasma (~ 30 μg/mL in adenomas or ~50 μg/mL in carcinomas) (Choi et al., 2013). This result demonstrated a quantitative response to a range of LRG1 protein concentrations and, thus, this method can be used as a sensing technique in quantitative colon cancer biomarker LRG1 detection. Importantly, a strong linear correlation between the ΔR_{ct} value and LRG1 concentration was shown in the range of 0–0.25 μg/mL (inset of Fig. 3b). When LRG1 concentration greater than 5 μg/mL was applied on the sensor layer, the ΔR_{ct} value reached saturation.

3.6. Electrochemical performance with crude blood plasma from CRC patients

Efficient and non-invasive biosensor systems have been described as playing an important role in the early diagnosis of cancer for point-of-care tests (Choi et al., 2013; Hwang et al., 2016; Sole et al., 2014). Therefore, the applicability of a bioanalytical technique to crude blood or plasma is necessary for the rapid and accurate diagnosis of cancer. EIS was performed using crude plasma from both adenoma patients ($n = 20$) and carcinoma patients ($n = 20$), and the change of impedance before and after the addition of plasma samples was measured (Fig. 5a). The data, as analyzed by 2-way ANOVA ($p < 0.001$) demonstrated a significantly different ΔR_{ct} between adenoma and carcinoma groups with our sensor system. The mean value of ΔR_{ct} for the adenoma group was 462.82, and that for the carcinoma group was 1926.15. The relative standard deviations (RSD) in the adenoma and carcinoma groups were found to be 45.2% and 24.5%, respectively. As shown in Fig. 5a, the ΔR_{ct} value measured by EIS with plasma samples of each patient ($n = 20$) from the same group was different. Because biomarker protein levels are highly patient-dependent and may vary for each patient. According to previous studies (Choi et al., 2013), LRG1 proteins were present in adenomas, but at lower concentrations than in carcinomas. In fact, the ΔR_{ct} values with adenoma and carcinoma plasma samples incubated on a gold electrode surface layer showed little variation in impedance change (Fig. 5a). On the other hand, the relative ΔR_{ct} value in crude human plasma was much higher than for the addition of pure LRG1 proteins. This might be due to the complexity of biological samples, which include various components that may influence the nature of affinity peptide binding. Non-specific binding to a small fraction of gold surface in the total sensor layer can lead to a mass change of impedance due to surface blocking. The calculated values of ΔR_{ct} and LRG1 protein concentrations in both patient groups as measured by our sensor system are shown in Table 1.

3.7. Stability of electrochemical sensor

The stability of the developed sensor was studied after immobilization of LRG1 BP3 peptides on a gold electrode and storage for 3 h. The experiment was carried out as follows: LRG1 BP3 peptides were immobilized on a gold electrode surface layer at room temperature and washed with PBS buffer. Afterwards, peptide-immobilized electrodes were kept for 3 h at room temperature. After incubation, pure LRG1, crude human plasma (adenomas and carcinomas), and PBS buffer as control were separately added onto a peptide-immobilized electrode, and the impedance change (ΔR_{ct} value) was measured. As observed from the results, the ΔR_{ct} value gradually decreased over the 3 h incubation period with crude plasma from carcinomas, which were

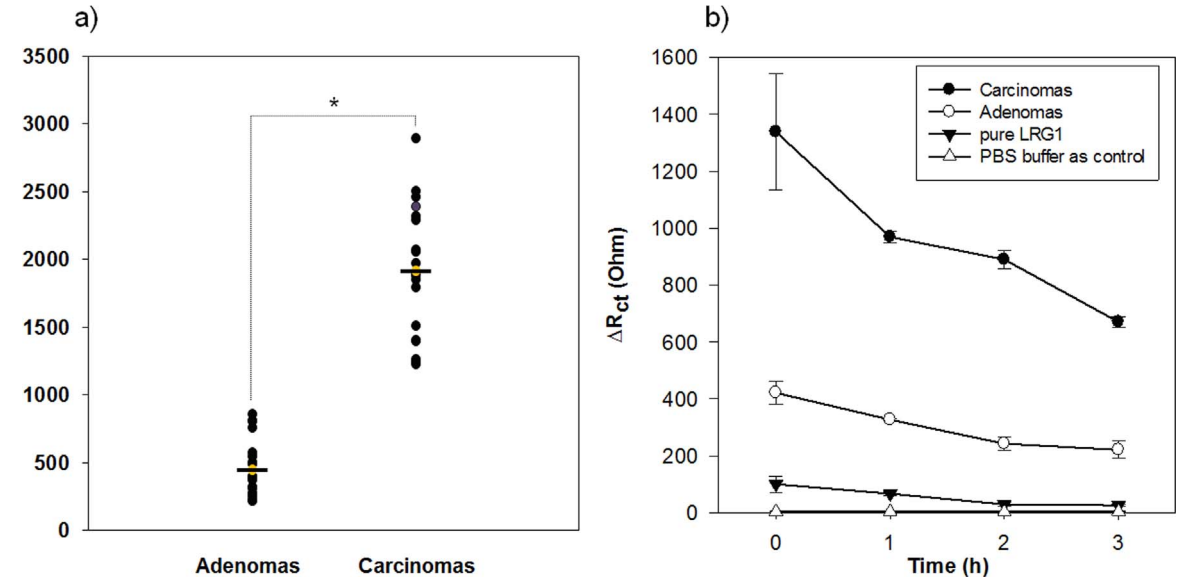

Fig. 5. Electrochemical sensor operation (a); the binding behavior of LRG1 BP3 peptides was significantly different by 2-way ANOVA (*$p < 0.001$). Stability of the sensor with impedance change (ΔR_{ct} value) measured by EIS (b). Each dot represents the mean value of a duplicated measurement. Mean values of group are indicated with bold lines.

Table 1
The average value of ΔR_{ct} and real LRG1 concentration in the crude plasma of adenoma and carcinoma patients measured by our sensor system.

Sample number	Sample type	Cancer type	Average ΔR_{ct}[a]	LRG1 concentration in crude plasma (μg/mL)[b]
1	Plasma	Carcinoma	1980.95	6.81 ± 0.36
2	Plasma	Carcinoma	2053.15	7.06 ± 0.85
3	Plasma	Carcinoma	1783.25	6.13 ± 0.49
4	Plasma	Carcinoma	2661.16	9.16 ± 0.91
5	Plasma	Carcinoma	1383.76	4.75 ± 0.68
6	Plasma	Carcinoma	1903.89	6.54 ± 0.51
7	Plasma	Carcinoma	2167.39	7.45 ± 0.53
8	Plasma	Carcinoma	1688.26	4.75 ± 0.63
9	Plasma	Carcinoma	1418.36	4.87 ± 0.52
10	Plasma	Carcinoma	2122.50	7.30 ± 1.36
11	Plasma	Carcinoma	1620.00	5.56 ± 1.17
12	Plasma	Carcinoma	2093.25	7.20 ± 1.14
13	Plasma	Carcinoma	1301.16	4.46 ± 0.49
14	Plasma	Carcinoma	2273.35	7.82 ± 1.01
15	Plasma	Carcinoma	1286.50	4.41 ± 0.56
16	Plasma	Carcinoma	2277.20	7.83 ± 1.16
17	Plasma	Carcinoma	1238.70	4.25 ± 0.39
18	Plasma	Carcinoma	1776.65	6.10 ± 1.01
19	Plasma	Carcinoma	1769.07	6.08 ± 0.17
20	Plasma	Carcinoma	2549.24	8.77 ± 0.40
21	Plasma	Adenoma	307.86	1.03 ± 0.09
22	Plasma	Adenoma	240.68	0.80 ± 0.07
23	Plasma	Adenoma	181.98	0.59 ± 0.25
24	Plasma	Adenoma	255.85	0.85 ± 0.63
25	Plasma	Adenoma	721.84	2.46 ± 0.44
26	Plasma	Adenoma	578.58	1.96 ± 0.07
27	Plasma	Adenoma	276.52	0.92 ± 0.53
28	Plasma	Adenoma	641.97	2.18 ± 0.45
29	Plasma	Adenoma	750.13	2.56 ± 0.49
30	Plasma	Adenoma	260.22	0.86 ± 0.72
31	Plasma	Adenoma	483.32	1.64 ± 0.73
32	Plasma	Adenoma	188.10	0.62 ± 0.16
33	Plasma	Adenoma	724.65	2.47 ± 0.38
34	Plasma	Adenoma	413.33	1.39 ± 0.72
35	Plasma	Adenoma	367.52	1.24 ± 0.13
36	Plasma	Adenoma	369.67	1.34 ± 0.80
37	Plasma	Adenoma	325.26	1.09 ± 0.40
38	Plasma	Adenoma	795.67	2.71 ± 0.29
39	Plasma	Adenoma	398.01	1.34 ± 0.05
40	Plasma	Adenoma	358.78	1.20 ± 0.39

[a] All measurements were done in triplicate.
[b] The LRG1 protein concentration was determined by the linear calibration curve (R^2 = 0.9844) in the inset data of Fig. 4b. Values are expressed as mean ± standard error, n = 3 in all cases.

much higher than the other two samples (pure LRG1 protein and plasma from adenomas) (Fig. 5b). The stability of the sensor was affected when two human plasma samples were added. This may, again, be due to the complicated biological matrix that included various components. However, a statistically significant difference between colorectal adenomas and carcinomas was observed, indicating that the sensor system was still active for diagnosing the adenoma-carcinoma transition with crude human plasma. As expected, there is no response in PBS buffer as control. Despite this, our method must still be optimized to improve the stability of the sensor and the storage lifetime. It is also of note that, although the sensitivity of our sensor appears to be fairly non-competitive in crude human plasma, the peptide-based sensor could be adaptable to a simple and miniaturized microdevice, thus developing a sensitive and label-free electrochemical biosensor in point-of-care diagnosis.

4. Conclusions

Herein, we demonstrate a general method for the development of an electrochemical peptide sensor using synthetic affinity peptides identified by phage display toward monitoring the adenoma-to-carcinoma transition in colon cancer. The whole process developed in this study includes as follows (Fig. S1); i) the selection of a target biomarker (LRG1), ii) biopanning of a phage displayed library to screen affinity peptides (Hwang et al., 2016), iii) synthesis of affinity peptides with a cysteine (LRG1 BP1–BP4), iv) in-situ monitoring of peptide immobilization, v) development of the biosensor, and vi) evaluation of the biosensor performance (specificity, sensitivity and stability) with electrochemical techniques (CV and EIS). The electrochemical peptide sensor had an equilibrium dissociation constant (K_d) of 8.3 ± 2.7 nM, which is below the physiological environmental condition of the target protein in colon cancer-related human plasma. The applicability of the sensor to detect LRG1 proteins from human plasma samples showed a statistically significant difference ($p < 0.001$) between adenomas and carcinomas. As only LRG1 protein was used as the target, and the performance of the sensor was validated for detection of the same protein, some other CRC biomarker proteins were present in the crude plasma of adenoma and carcinoma patients and, therefore, further validation of our sensor using these biomarker proteins is needed. The comparison of analytical performance for the detection of colon cancer was shown in Table S3. Based on these observations, this general strategy for sensor development for point-of-care diagnosis is straightforward and can be applied in monitoring colorectal adenoma-to-carcinoma progression or other cancer-related assays. Furthermore, there are many advantages that create a sensitive and potent diagnostic biosensor for clinical and medical applications.

Acknowledgements

This study was supported by a grant from the National Research Foundation of Korea (NRF) funded by the Korea government (MSIP) (NRF-2014R1A2A2A01005621, NRF-2017R1A2A2A05001037).

Appendix A. Supplementary material

Supplementary data associated with this article can be found in the online version at doi:10.1016/j.bios.2017.07.013.

References

Abdolahad, M., Shashaani, H., Janmaleki, M., Mohajerzadeh, S., 2014. Biosens. Bioelectron. 59, 151–159.
Albrethsen, J., Bøgebo, R., Gammeltoft, S., Olsen, J., Winther, B., Raskov, H., 2005. BMC Cancer 5, 1–10.
Choi, J.W., Liu, H., Shin, D.H., Yu, G.I., Hwang, J.S., Kim, E.S., Yun, J.W., 2013. Proteomics 13, 2361–2374.
Clark-Langone, K.M., Wu, J.Y., Sangli, C., Chen, A., Snable, J.L., Nguyen, A., Hackett, J.R., Baker, J., Yothers, G., Kim, C., Cronin, M.T., 2007. BMC Genom. 8, 279–296.
Crivianu-Gaita, V., Thompson, M., 2016. Biosens. Bioelectron. 85, 32–45.
Daniels, J.S., Pourmand, N., 2007. Electroanalysis 19, 1239–1257.
Galamb, O., Sipos, F., Spisak, S., Galamb, B., Krenacs, T., Valcz, G., Tulassay, Z., Molnar, B., 2009. Cell. Oncol. 31, 19–29.
Giusti, L., Iacconi, P., Da Valle, Y., Ciregia, F., Ventroni, T., Donadio, E., Giannaccini, G., Chiarugi, M., Torregrossa, L., Proietti, A., Basolo, F., Lucacchini, A., 2012. Mol. Biosyst. 8, 1088–1099.
Grewal, Y.S., Shiddiky, M.J.A., Spadafora, L.J., Cangelosi, G.A., Trau, M., 2014. Biosens. Bioelectron. 55, 417–422.
Hu, R., Wen, W., Wang, Q., Xiong, H., Zhang, X., Gu, H., Wang, S., 2014. Biosens. Bioelectron. 53, 384–389.
Hwang, H.J., Ryu, M.Y., Lee, G.B., Park, J.P., 2016. ChemistrySelect 1, 1140–1143.
Hwang, H.J., Ryu, M.Y., Park, C.Y., Ahn, J., Park, H.G., Choi, C., Ha, S.-D., Park, T.J., Park, J.P., 2017. Biosens. Bioelectron. 87, 164–170.
Hwang, H.J., Ryu, M.Y., Park, J.P., 2015. RSC Adv. 5, 55300–55302.
Ihi, T., Nakazato, M., Mukae, H., Matsukura, S., 1997. Clin. Infect. Dis. 25, 1134–1140.
Kehoe, J.W., Kay, B.K., 2005. Chem. Rev. 105, 4056–4072.
Kolitz-Domb, M., Grinberg, I., Corem-Salkmon, E., Margel, S., 2014. J. Nanobiotechnol. 12, 1–13.
Kumar, S., Dimmock, J.R., Sharma, R.K., 2011. Cancers 3, 1372–1382.
Li, T., Leong, M.H., Harms, B., Kennedy, G., Chen, L., 2013. World J. Gastroenterol. 19, 5615–5621.
Park, J.P., Cropek, D.M., Banta, S., 2010. Biotechnol. Bioeng. 105, 678–686.
Park, J.P., Park, C.Y., Park, A.Y., Ryu, M.Y., 2015. RSC Adv. 5, 90531–90533.
Rangiah, K., Tippornwong, M., Sangar, V., Austin, D., Tetreault, M.P., Rustgi, A.K., Blair,

I.A., Yu, K.H., 2009. J. Proteome Res. 8, 5153–5164.
Schoen, R.E., 2002. Nat. Rev. Cancer 2, 65–70.
Sidhu, S.S., 2001. Biomol. Eng. 18, 57–63.
Sole, X., Crous-Bou, M., Cordero, D., Olivares, D., Guino, E., Sanz-Pamplona, R., Rodriguez-Moranta, F., Sanjuan, X., de Oca, J., Salazar, R., Moreno, V., 2014. PLoS One 9, e106748.
Tao, L., Zhang, K., Sun, Y., Jin, B., Zhang, Z., Yang, K., 2012. Biosens. Bioelectron. 35, 186–192.
Wu, J., Cropek, D.M., West, A.C., Banta, S., 2010. Anal. Chem. 82, 8235–8243.
Wu, J., Park, J.P., Dooley, K., Cropek, D.M., West, A.C., Banta, S., 2011. PLoS One 6, e24948.
Wu, L., Qu, X., 2015. Chem. Soc. Rev. 44, 2963–2997.
Yi, J.M., Dhir, M., Guzzetta, A.A., Iacobuzio-Donahue, C.A., Heo, K., Yang, K.M., Suzuki, H., Toyota, M., Kim, H.M., Ahuja, N., 2012. Tumour Biol. 33, 363–372.
Zhang, Y., Chen, J., Hu, Z., Hu, D., Pan, Y., Ou, S., Liu, G., Yin, X., Zhao, J., Ren, L., Wang, J., 2007. J. Biomol. Screen. 12, 429–435.